Pterodactyl: Coupled 6-DOF Integration of Guidance and Control Algorithms in Genesis

Zarrin T. Bashir[1] and Quincy E. McKown[2]
Analytical Mechanics Associates, Inc., Moffett Field, CA 94035

Sarah N. D'Souza[3] and Benjamin W. L. Margolis[4]
NASA Ames Research Center, Moffett Field, CA 94035

Breanna J. Johnson[5]
NASA Johnson Space Center, Houston, TX 77058

The NASA-funded Pterodactyl project seeks to advance the current state-of-the-art for entry vehicles by developing novel guidance and control technologies for Deployable Entry Vehicles (DEVs). This paper builds upon the Pterodactyl architecture that employed eight individually articulating flaps with two options for guidance, bank angle modulation with the Fully Numerical Predictor Corrector Entry Guidance technique (FNPEG) and angle of attack and sideslip modulation with FNPEG uncoupled range control (FNPEG URC). These, with a linear quadratic regulator (LQR) controller, had previously been presented in uncoupled 3-DOF trajectories. This work will show results from fully coupled 6-DOF simulations, leveraging recent advancements in trajectory simulation software, namely the Julia-based Genesis package. Preliminary results show good performance for angle of attack and sideslip modulation when using a controller designed at high dynamic pressure conditions.

I. Nomenclature

ADEPT	=	Adaptive Deployable Entry and Placement Technology
DEV	=	Deployable Entry Vehicle
DOF	=	Degree(s) of Freedom
FNPEG	=	Fully Numerical Predictor-corrected Entry Guidance
FNPEG URC	=	Fully Numerical Predictor-corrected Entry Guidance Uncoupled Range Control
GNC	=	Guidance Navigation and Control
HIAD	=	Hypersonic Inflatable Aerodynamic Decelerator
LQR	=	Linear Quadratic Regulator
PBV	=	Pterodactyl Baseline Vehicle
A	=	state matrix
B	=	control input matrix
K	=	feedback gain matrix
M	=	Mach number
Q	=	state diagonal weighting matrix
R	=	control input diagonal weighting matrix

[1] Aerospace Engineer Intern, Entry Systems and Vehicle Development Branch, AIAA Member.
[2] Aerospace Engineer, Entry Systems and Vehicle Development Branch, AIAA Member.
[3] Principal Investigator, Entry Systems and Vehicle Development Branch, AIAA Member.
[4] Aerospace Engineer, Systems Analysis Office, NASA ARC/AA.
[5] Aerospace Engineer, Flight Mechanics and Trajectory Design Branch, NASA JSC/EG5, AIAA Member.

e	=	normalized specific mechanical energy
e_i	=	integral error state of term *i*
p	=	roll rate
q	=	pitch rate
q_∞	=	freestream dynamic pressure
r	=	yaw rate
r_{dist}	=	planetocentric radial distance
u	=	control input vector
V_∞	=	freestream velocity
x	=	state vector
α	=	angle of attack (alpha)
β	=	sideslip angle (beta)
δ	=	flap deflection angle
Δ	=	deviation
ρ_∞	=	freestream density
σ	=	bank angle

Superscripts

^{T}	=	transpose
$\dot{}$	=	first derivative
*	=	linearization point

Subscripts

$_{1-8}$	=	flap number
$_c$	=	commanded value

II. Introduction

As the scope of planetary exploration continues to expand, achieving the bold science objectives will require precision landing site targeting and novel heatshield technologies. To address these needs, NASA has invested in Deployable Entry Vehicle (DEV) technologies, such as the Adaptable, Deployable, Entry Placement Technology (ADEPT) [1] and hypersonic inflatable aerodynamic decelerator (HIAD) technology [1]. The NASA Pterodactyl project seeks to investigate novel guidance and control technologies for said Deployable Entry Vehicles. Previous work has investigated three candidate control architectures including a flap control system, mass movement control system, and a reaction control system, where the flap control system was identified as the most promising as it allocated more payload volume and provided increased maneuverability [3]. Original guidance and control algorithms were developed to advance the capabilities of the flap control system. The first of these, "alpha-beta", employs a linear quadratic regulator (LQR) controller, which modulates angle of attack and sideslip angle couples with Fully Numerical Predictor-corrected Entry Guidance Uncoupled Range Control (FNPEG URC) [4]. The second of these, "yaw-to-bank", also employs an LQR controller, which instead modulates the yaw angle to achieve bank control, couples with Fully Numerical Predictor-corrected Entry Guidance (FNPEG) [4].

Previously published work on the alpha-beta control and yaw-to-bank control utilized uncoupled three degree-of-freedom (3-DOF) trajectory simulations. The work presented here integrates the guidance and control algorithms in a coupled six degree-of-freedom (6-DOF) trajectory simulation for both controller schemes. The outline of the paper is as follows: the case study, which is the same lunar sample return mission to Earth as presented in previous Pterodactyl publications, is described. This is followed by details on the vehicle architecture and configuration. Next, a brief overview on the control and guidance system designs is provided. Then a description of the 6-DOF simulation tool is given. Results of simulations are then shown, followed by concluding remarks.

III. Methodology

This work seeks to build upon the foundational control and guidance algorithms developed by Margolis, Johnson, and Okolo by combining these guidance and control systems in a 6-DOF trajectory simulation [4-6]. These original methods were derived and presented using uncoupled 3-DOF simulations for an ADEPT vehicle with eight deployable flaps. Two LQR control systems were derived: 1) simultaneous angle of attack and sideslip control ("alpha-beta") and 2) yaw modulation to achieve bank control ("yaw-to-bank").

First, the case study mission profile was replicated to the original study and consistency between the aerodynamic databases and vehicle configurations was confirmed. Then the control and guidance algorithms were implemented in the 6-DOF trajectory simulation software. Checkouts to confirm implementation were performed, such as open-loop (guidance off, control off) cases and constant commands with control on, guidance off. Finally, parameter tuning and gain scheduling were used to achieve better tracking with a pre-defined baseline guidance profile. Each of these will be described in detail in following sections.

A. Lunar Return Mission

The lunar return mission case study was employed to build on existing framework and maintain relevancy for current spaceflight endeavors [4]. The flap control system steers the vehicle to a desired target location simulated in the Utah Test and Training Range (UTTR). At an entry interface of 122 km, the velocity is 11.0 km/s, where the vehicle then decelerates to terminal descent conditions of Mach 2. This case does carry high Earth entry speeds and thus stresses the integrated flap system to maintain guidance commands.

B. PBV-II, PBV-IIa, and Aerodynamic Control Surface Architecture

The ADEPT Pterodactyl Baseline Vehicle (PBV) was used to match original development's configuration [4]. The PBV-II nomenclature implies a symmetric vehicle and is an iteration of the smaller, asymmetric PBV-I. PBV-II is shown in Figure 1 below. PBV-II has no longitudinal center of gravity offset, while PBV-IIa has a longitudinal center of gravity offset that enables a trim angle of attack (α_{trim}) of -14°, however the external configuration is shared and both vehicles are represented by Figure 1. The mass and moment of inertia properties of PBV-II and PBV-IIa are shown in Table 1. The flap capabilities and bounding conditions are the same as the previous study: eight individually actuated flaps with an operating range of +20° into the flow and -45° out of the flow with a shared initial condition of -35°. For the angle of attack and sideslip control architecture, the lateral flaps (3-6) are intended to modulate the sideslip angle, whereas the longitudinal flaps (1-2, 7-8) alter the angle of attack angle.

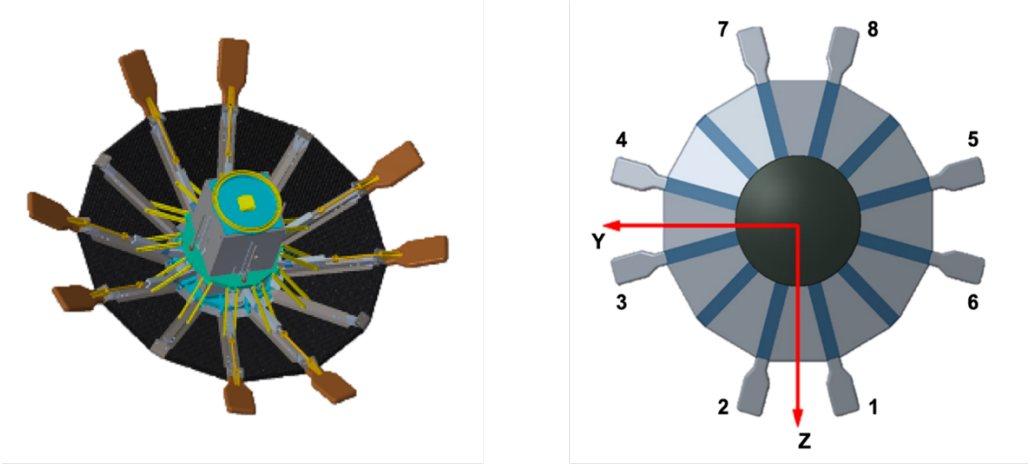

Figure 1: (a.) PBV-II Aft View, (b.) PBV-II Forebody View

Table 1: Vehicle Properties of PBV-II and PBV-IIa

Parameter	Units	PBV-II	PBV-IIa
Mass	kg	703.3	702.4
Ixx	kg-m^2	651.2	693.7
Iyy	kg-m^2	513.4	572.2
Izz	kg-m^2	512.9	512.0
Ixy = Iyz	kg-m^2	0	0
Ixz = Izx	kg-m^2	0	-35.23
CG measured from nose	[m, m, m]	[-0.458, 0, 0]	[-0.469, 0, -0.079]

C. Control System Design

The specifics of the control system are described in Margolis, et. al. [4] and Okolo, et. al. [5] with a summary of the linear quadratic regulator (LQR) system provided here. With the vehicle attitude state vector, x, and the control input vector, u, the equations of motion are linearized to generate a linear controller, with the resultant state-space linear equations taking the form:

$$\Delta\dot{x} = A\,\Delta x + B\,\Delta u$$

where Δx and Δu are the deviations from the linearization point x^* and u^* with the state matrix, A, and the input matrix, B, defined by

$$A = \left.\frac{\partial f}{\partial x}\right|_{x^*u^*}$$

$$B = \left.\frac{\partial f}{\partial u}\right|_{x^*u^*}$$

where $f(x,u)$ is the vector-valued function of the derivatives for each state variable concatenated together, and the vehicle state vector, x, is defined as

$$x = [p\ q\ r\ \sigma\ \alpha\ \beta\ e_\sigma\ e_\alpha\ e_\beta]^T$$

and the control input vector, u, is expressed as

$$u = [\delta_1\ \delta_2\ \ldots\ \delta_7\ \delta_8]^T$$

where e_σ, e_α, and e_β are the augmented integral error state variables for σ, α, and β, respectively, and each δ_i is the deflection of the ith flap. The vehicle state defined above is the augmented state associated with the attitude, and it is largely de-coupled form the translational state. The linearization point assumes steady-state conditions, zero integral error ($\bar{e} = 0$), symmetric nominal control surface deflections, and trim angle of attack from a Newton-Raphson solver. To start, the control system was designed around flight conditions at the altitude that activated guidance and control as provided by the guidance simulation. The control law is then given by

$$u = u^* - K(x - x_c)$$

where x_c is the commanded state, and K, the feedback gain matrix, is computed to minimize the quadratic cost functional defined as

$$J = \int_0^\infty \Delta x^T(\tau)\,Q\,\Delta x(\tau) + \Delta u^T(\tau)\,R\,\Delta u(\tau)\,d\tau$$

and is calculated using either Algebraic Riccati Equation or Linear Matrix Inequality depending on the case. The matrices Q and R, diagonal weighting matrices for the states and control surfaces, respectively, are tuned by evaluating performance and control effort. The feedback gain matrix K is tuned to improve tracking by updating the flight conditions, namely freestream dynamic pressure, q_∞, via fluid freestream density, ρ_∞, and freestream vehicle velocity, V_∞. The remaining parameters are held constant.

D. Guidance System Design

The guidance system design is defined in detail in Johnson, et. al. [6], but a short overview is given here. The guidance algorithm for angle of attack and sideslip employs FNPEG URC and FNPEG for yaw-to-bank as was conducted in the baseline study [4]. FNPEG URC generates angle of attack (α) and sideslip angle (β) commands to alter the vehicle's lift and drag vectors assuming a fixed bank angle. FNPEG generates bank angle (σ) commands to roll the vehicle's total lift vector assuming a fixed angle of attack profile. Recall that the vehicle configuration for yaw-to-bank, PBV-IIa, possesses a longitudinal center of gravity offset, generating a trim angle of attack (α_{trim}) and a non-zero lift vector. Both employ the Gauss-Newton method within the predictor-corrector logic to search for the best command angle magnitude versus energy profile to achieve a minimal miss distance [6]. This energy profile is represented by *e.*

The negative of the normalized specific mechanical energy, e, is

$$e = \frac{1}{r_{dist}} - \frac{V^2}{2}$$

where r_{dist} is the planetocentric radial distance to the vehicle and V is the planet-relative velocity. The alpha-magnitude profile for FNPEG URC is defined as

$$|\alpha(e)| = \alpha_0 + \frac{e - e_0}{e_f - e_0}(\alpha_f - \alpha_0)$$

This alpha-magnitude profile, $|\alpha(e)|$, is parameterized by a linear function of the normalized specific mechanical energy, e. FNPEG URC's, like FNPEG's, numerical method solves a least-squares problem with a single univariate function to find the α_0 needed to minimize the error function defined as

$$f(\alpha_0) = \frac{1}{2}\left[S_{togo}(e_f)\right]^2$$

where S_{togo} defines the great-circle range to the target site. The calculated α_0 and e_0 are used to predict the resultant trajectory within each prediction-correction cycle, and if the calculated α_0 does not meet the terminal constraint on the error of the range to target, then the Gauss-Newton scheme corrects the trajectory by updating α_0 until the error of the range to target is within limits. A corresponding procedure is defined for FNPEG guidance with σ instead of α.

In short, both FNPEG URC and FNPEG necessitate a user-defined control angle at a target energy to determine an angle profile linear with respect to energy. This angle profile is then used in the predictor-corrector throughout flight [6]. It has been observed that both FNPEP URC and FNPEG have fast and reliable convergence rates.

E. Integrated 6-DOF Simulation

This work leverages the 6-DOF trajectory capabilities of the Genesis design tool instantiated in Julia [7]. Using the 6-DOF translational and rotational equations of motion defined in Genesis, and a 100 Hz Runge-Kutta 4 integration scheme, the control and guidance algorithms are implemented in the simulation using a `FlightSoftwareRateGroup` at a prescribed rate. The pre-defined aerodynamic database, with dependence on Mach number (M), angle of attack (α), sideslip angle (β), and each deflection angle (δ_i), alter the vehicle's forces and moments at each time step according to the controlled-to flap deflection configuration and current state parameters. The trajectory of the vehicle is determined, and the impact location is compared to the target site, along with target parameter tracking for each respective control algorithm.

IV. Results

A. Implementation of Integrated 6-DOF Simulation with Angle of Attack and Sideslip Control (alpha-beta) and FNPEG URC Guidance

The successful implementation of the alpha-beta 6-DOF simulation involved (1.) the verification and integration of the aerodynamics module, or `PteroAero`, that outputs aerodynamic force and moment coefficients of the vehicle into the Genesis trajectory simulation, (2.) the verification and integration of the controller module, or `PteroController`, which ingests the state of the vehicle at a point in time, and returns a gain matrix, or `Kmat`, to stabilize the vehicle (referenced in Section III.C as K), and lastly (3.) testing the tracking of the guidance and commanded outputs of the angle of attack (α) and sideslip angle (β) after complete integration. In each of these verification scenarios, the full 6-DOF dynamics were integrated with initial conditions as described in Section III.A, vehicle parameters as provided in Table 1, and simulated for a specified time of 100 seconds to assess the integrated simulation.

1. *Open Loop* Case

The aerodynamics inputs come in the form of a Julia based module, `PteroAero.jl`, which intakes aerodynamic coefficients across Mach, vehicle angle of attack, vehicle sideslip angle, and eight flap deflection angles. This data is sourced from previously performed Cart3D simulations, which provides computational fluid dynamics analysis for preliminary aerodynamics design. The module then interpolates the aerodynamic moment and force coefficients, and outputs the resulting coefficients per function query [8]. This module is used in both the alpha-beta and yaw-to-bank simulations. Prior to the integration of guidance or control , the aerodynamics module was implemented and validated by running the 6-DOF simulation with no controller or guidance active, and by manually setting all the eight flaps' deflections of the vehicle to 0°. The response in Figure 2 shows that the angle of attack and side slip angle holds at 0° throughout the simulation, which was the expected result. This validates that the aerodynamics was integrated correctly.

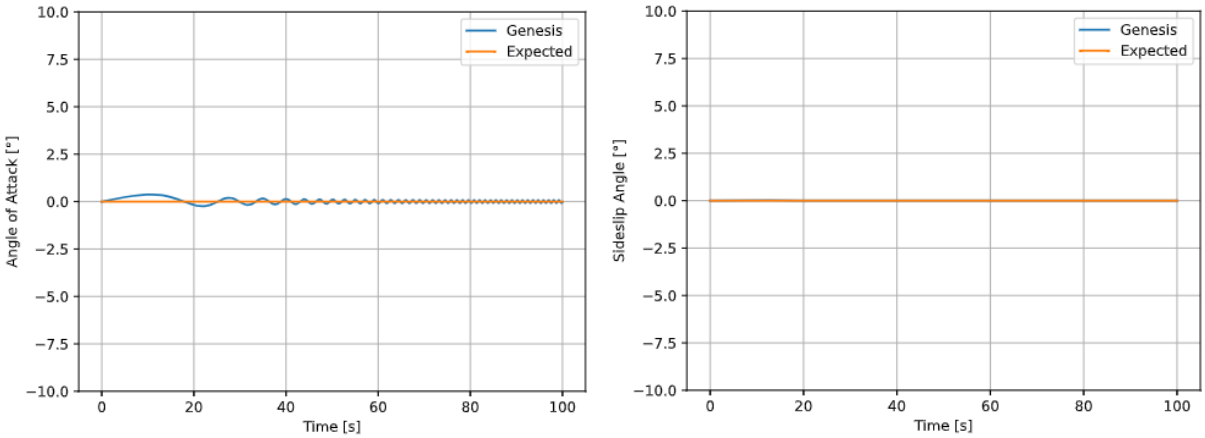

Figure 2: Angle of Attack and Side Slip Angle Responses in Open Loop Case

2. *Hold Command Case(s)*

Once the aerodynamics was established and deemed accurate, the integration and verification of the controller took place. The controller is in the form of a Julia based module, `PteroController.jl`, which consists of the original controller algorithm translated to Julia. To verify the implementation of the alpha-beta controller, it was tested in isolation, turning the guidance off, and using manual hold values for the commanded angle of attack and sideslip angle. The hold commands tested were from within the control envelope [4]. The responses showed that the controller was able to hold at the *commanded* values of both the angle of attack (α_c) and sideslip angle (β_c). This validates that controller was integrated correctly. Examples of these are shown in Figure 3 , Figure 4, and Figure 5.

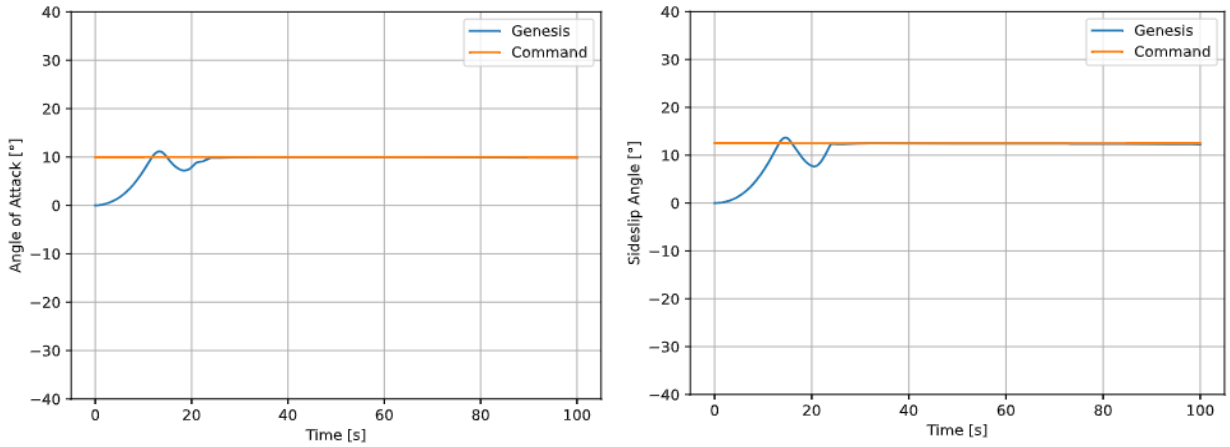

Figure 3: Angle of Attack and Side Slip Angle Responses in Hold Response Case, where α_c = 10° and β_c= 12.5°

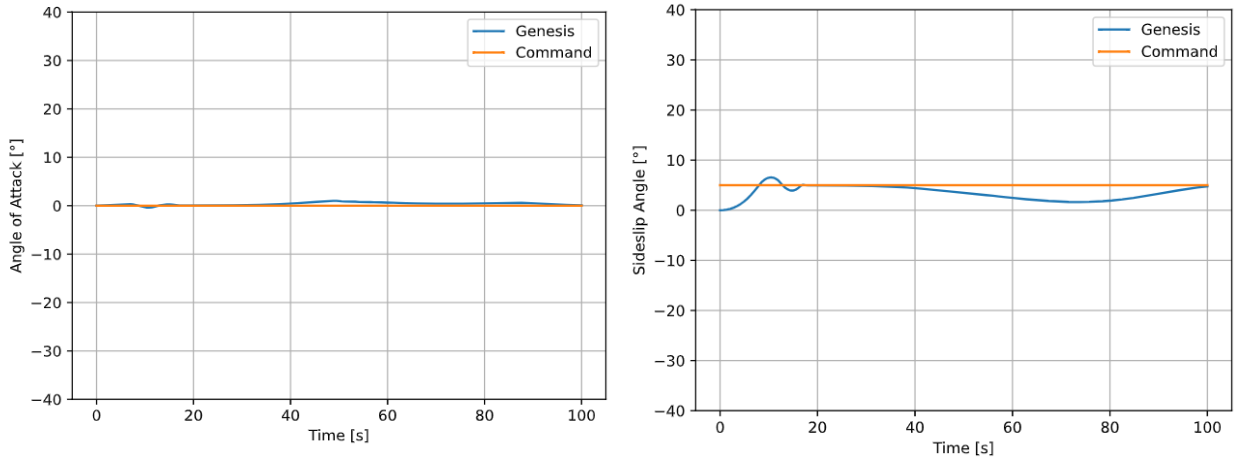

Figure 4: Angle of Attack and Side Slip Angle Responses in Hold Response Case, where α_c = 0° and β_c= 5°

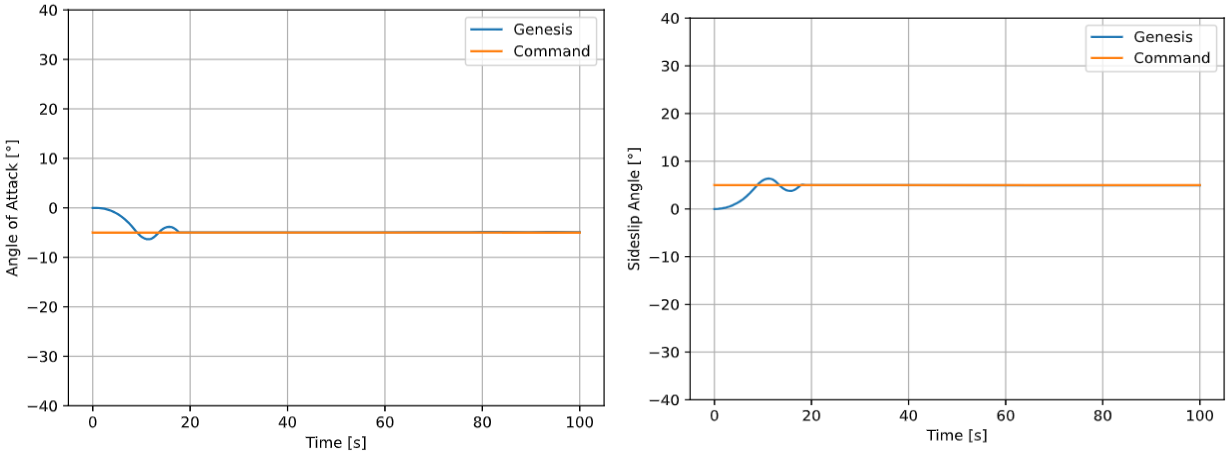

Figure 5: Angle of Attack and Side Slip Angle Responses in Hold Response Case, where α_c= -5° and β_c= 5°

3. Guidance On, Control On

To determine the performance of the integrated 6-DOF guidance and control for alpha-beta control, both guidance and control were turned on and active in the simulation as a respective `FlightSoftwareRateGroup` in Genesis. The response in Figure 6 shows that the guided and commanded values were nearly aligned and tracking throughout the simulation. The close tracking between the commanded guidance values and the simulated response values indicates that the integration of the alpha-beta LQR controller and corresponding FNPEG URC guidance into Genesis was completed accurately.

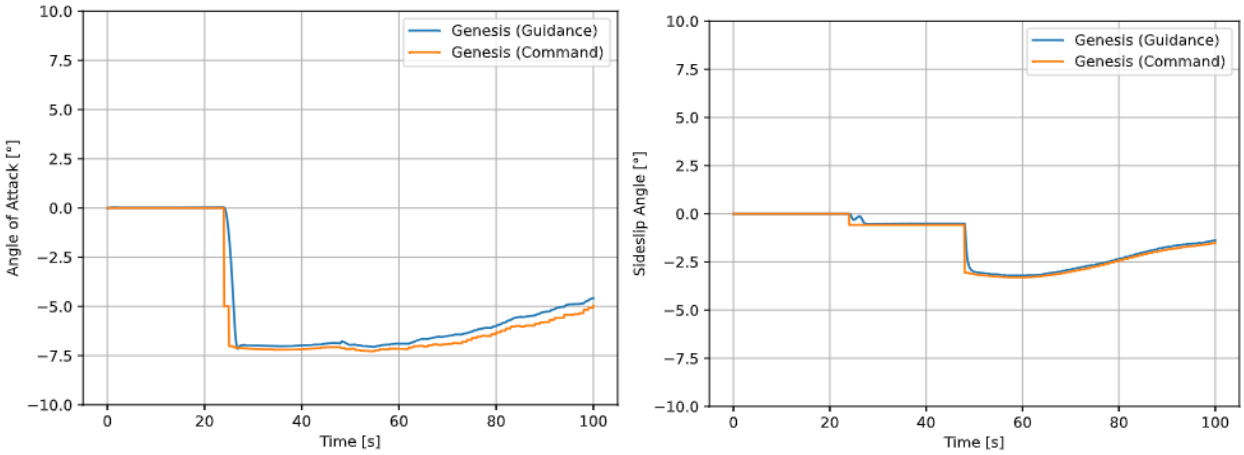

Figure 6: Angle of Attack and Side Slip Angle Responses in Guidance on, Control on Case

However, the slight misalignments in the tracking in the integrated simulation shown in Figure 6, particularly after 60 seconds for angle of attack, indicate a need for further tuning of the controller. Additional simulation time is necessary to determine the target miss distance and propagate the vehicle state to the surface. The main parameter of tuning the controller is adjusting the gain matrix, or `Kmat`. The `Kmat` is generated using cost parameters and a specific condition of the trajectory, namely dynamic pressure controlled by velocity and density. Results shown above were generated with a `Kmat` derived with a high dynamic pressure and relatively low altitude. Iterations with different `Kmat`'s to achieve better tracking, along with gain scheduling, are currently being investigated.

B. Implementation of Integrated 6-DOF Simulation with Yaw-To-Bank Control and FNPEG Guidance

The process of implementing the yaw-to-bank LQR controller into Genesis is like that of the alpha-beta LQR controller process described above. In each of the verification scenarios, the full 6-DOF dynamics were integrated, starting at the initial conditions described in Section III.A, using vehicle parameters for PBV-IIa in Table 1, and simulated for a specified time of 100 seconds to assess the integrated simulation. The key differences between the two implementations are the Pterodactyl vehicle model, the gain matrices used in the controller (for yaw-to-bank, these are `K_ab` and `K_bank`), and the guidance output, which is now bank angle. Lessons learned through the implementation of the alpha-beta implementation will be incorporated in the yaw-to-bank counterpart. The implementation of the yaw-to-bank simulation is currently underway and the following are preliminary results.

1. Open Loop Case

Identical to an open loop case in the alpha-beta simulation, this case was run by turning both the guidance and control off and by manually setting all the eight flap's deflections to zero. However, for a yaw-to-bank open loop case, it is expected that the angle of attack response will hold at the trim angle value, 14° because of a center of gravity offset, and the bank angle value should hold to 0°. Results for this are shown in Figure 7 and Figure 8.

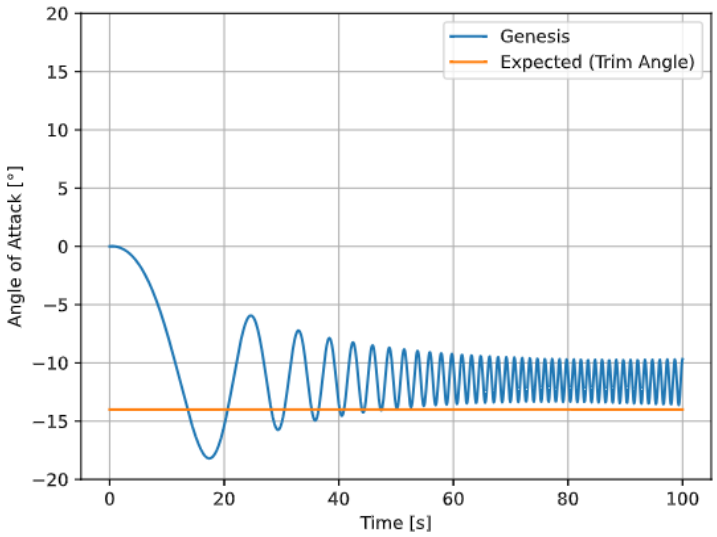

Figure 7: Angle of Attack Response in Open Loop Case

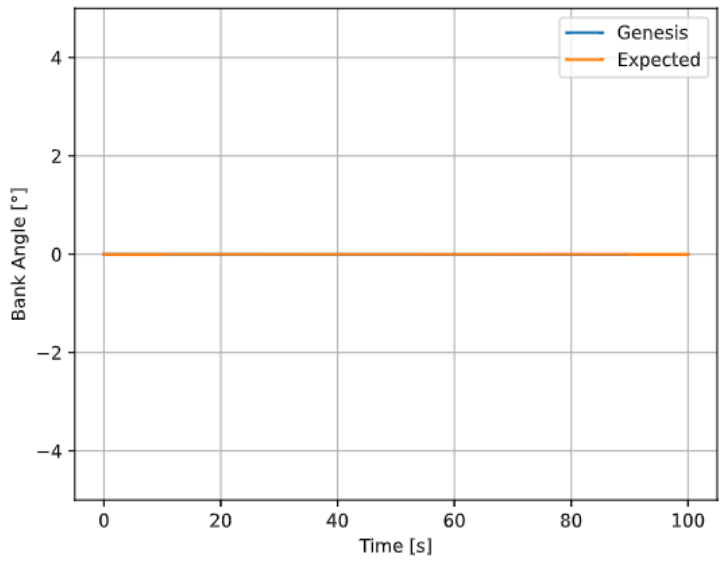

Figure 8: Bank Angle Response in Open Loop Case

2. Hold Command Case

To test the implementation of the yaw-to-bank controller, the controller was tested in isolation by turning the guidance off and using manual hold commands for the commanded bank angle. The angle of attack commanded value was set to a constant value of the trim angle (-14°). The response shown in Figure 9 reveals that the controller was approximately able to hold at the commanded bank angle (σ_c) with some deviation towards the end of the simulation. This indicated that the controller needs to be tuned to improve tracking for the bank angle.

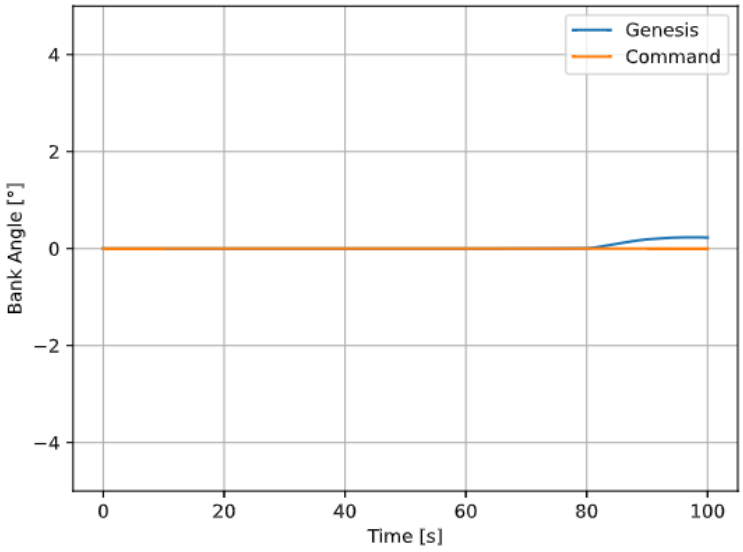

Figure 9: Bank Angle Response in Hold Command Case, where σ_c= 0°

3. Guidance On, Control On

The unaligned tracking between the Genesis simulated guidance and commanded values in Figure 10 indicates that the integration of the yaw-to-bank controller into Genesis needs to be further investigated.

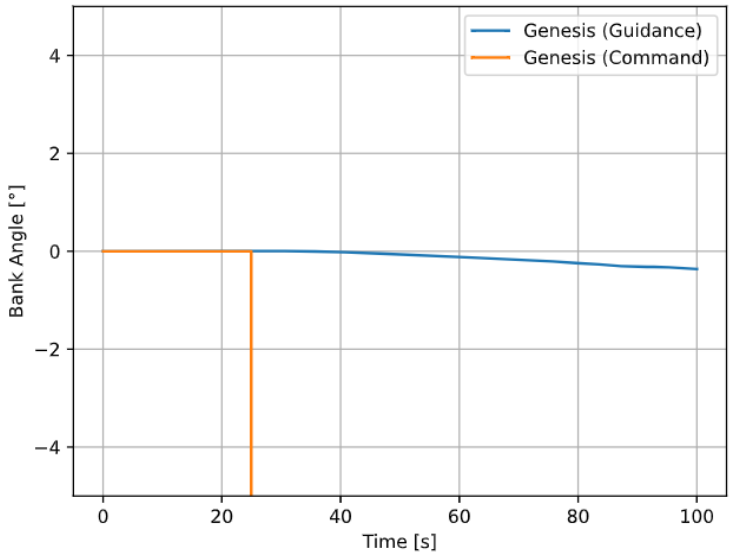

Figure 10: Bank Angle Response in Guidance on, Control on Case

V. Conclusions

Two integrated guidance and control algorithms in a 6-DOF trajectory simulation for a deployable vehicle with eight individually articulating flaps were presented. Angle of attack and sideslip control (alpha-beta) showed promising results with suitable tracking against guidance commands. Preliminary results indicate that gain scheduling provides no additional benefit to performance, where a controller derived at a high dynamic pressure condition showed the best performance. It may be noted that previous work in Margolis [4] with uncoupled 3-DOF simulations also did

not employ gain scheduling, and the best performing controller was derived at low dynamic pressure conditions. A controller derived at a low dynamic pressure condition conceivably employs greater control authority and generates more rapid individual responses from the flaps. From this, it may be inferred that additional control authority is necessary when the simulation incorporates additional degrees-of-freedom. Possible reasons include cross-coupling of terms to excite rotation modes not obvious in 3-DOF, energy transfer between degrees-of-freedom, and an overall more excited system. Finally, additional work is needed to tune the controller for yaw-to-bank.

Acknowledgments

The authors would like to thank the Entry Systems Modeling project for funding this work and continued commitment to Pterodactyl, as well as Antonella Alunni, Soumya Dutta, and Daniel Matz for their support.

References

[1] Venkatapathy, E., Hamm, K., Fernandez, I., Arnold, J., Kinney, D., Laub, B., Makino, A., McGuire, M., Peterson, K., Prabhu, D., Empey, D., Dupzyk, I., Huynh, L., Hajela, P., Gage, P., Howard, A., and Andrews, D., "Adaptive Deployable Entry and Placement Technology (ADEPT): A Feasibility Study for Human Missions to Mars," *21st AIAA Aerodynamic Decelerator Systems Technology Conference and Seminar*, AIAA 2011-2608, Dublin, Ireland, 2011.

[2] NASA/Space Technology Mission Directorate, "Hypersonic Inflatable Aerodynamic Decelerator," , 2014. URL https://www.nasa.gov/directorates/spacetech/game_changing_development/HIAD/index.html.

[3] Alunni, A. I., D'Souza, S. N., C., B., Okolo, W. A., Nikaido, B. E., Margolis, B. W., Johnson, B. J., Barton, J. D., Lopez, G., Wolfarth, L. S., and Hays, Z. B., "Pterodactyl: Trade Study for an Integrated Control System Design of a Mechanically Deployable Entry Vehicle," *AIAA SciTech 2020 Forum*, AIAA, Orlando, FL, 2020.

[4] Margolis, B. W., Okolo, W. A., D'Souza, S. N., and Johnson, B. J., "Pterodactyl: Guidance and Control of a Symmetric Deployable Entry Vehicle Using an Aerodynamic Control System," *AIAA SciTech 2021 Forum*, AIAA, Virtual, 2021.

[5] Okolo, W. A., Margolis, B. W., D'Souza, S. N., and Barton, J. D., "Pterodactyl: Development and Comparison of Control Architectures for a Mechanically Deployed Entry Vehicle," *AIAA SciTech 2020 Forum*, AIAA, Orlando, FL, 2020.

[6] Johnson, B. J., Rocca-Bejar, D., Lu, P., Nikaido, B. E., Yount, B. C., D'Souza, S. N., and Hays, Z. B., "Pterodactyl: Development and Performance of Guidance Algorithms for a Mechanically Deployed Entry Vehicle," *AIAA SciTech 2020 Forum*, AIAA, Orlando, FL, 2020.

[7] Murri, D. G., Matz, D. A., Hoffman, D. A., Berndt, J. S., Brown, S. C., and Prokop, L. E., "Improvements to the Flight Analysis and Simulation Tool (FAST) and Initial Development of the Genesis Flight Mechanics Simulation for Ascent, Aerocapture, Entry, Descent, and Landing (A2EDL) Trajectory Design," NASA/TM-20210014622, Apr 2021.

[8] Reddish, B. J., Nikaido, B. E., D'Souza, S. N., Hawke, V., and Kang, H., "Pterodactyl: Aerodynamic Modeling for a Symmetric Deployable Earth Entry Vehicle with Flaps," *AIAA SciTech 2021 Forum*, AIAA, Virtual, 2021.